Saudi Journal of Biological Sciences 27 (2020) 3434–3441

Contents lists available at ScienceDirect

Saudi Journal of Biological Sciences

journal homepage: www.sciencedirect.com

Original article

Green synthesis of silver nanoparticles using *Citrus limon* peels and evaluation of their antibacterial and cytotoxic properties

Manal M. Alkhulaifi [a], Jamilah H. Alshehri [a], Moudi A. Alwehaibi [a], Manal A. Awad [b], Nouf M. Al-Enazi [c], Noura S. Aldosari [a,*], Ashraf A. Hatamleh [a], Neveen Abdel- Raouf [c,d,*]

[a] Department of Botany and Microbiology, College of Science, King Saud University, Riyadh 11451, Saudi Arabia
[b] King Abdullah Institute for Nanotechnology, King Saud University, Saudi Arabia
[c] Department of Biology, College of Science and Humanities in Al-Kharj, Prince Sattam bin Abdulaziz University, Al-Kharj 11942, Saudi Arabia
[d] Botany and Microbiology Department, Faculty of Science, Beni-Suef University, Beni-Suef, 65211, Egypt

ARTICLE INFO

Article history:
Received 28 July 2020
Revised 11 September 2020
Accepted 15 September 2020
Available online 23 September 2020

Keywords:
Green Silver nanoparticles
Citrus limon peels
Antibacterial activity
Cytotoxic activity
Breast cancer
Carcinoma cell line

ABSTRACT

The present work aimed to synthesis silver nanoparticles (AgNPs) using biological waste products *Citrus limon* peels, its characterization, antimicrobial activities and the cytotoxic effect of the synthesized green AgNPs. Characterization of the prepared AgNPs showed the formation of spherical, and few agglomerated AgNPs forms as measured by UV–visible spectrophotometer. The average size of the prepared AgNPs was 59.74 nm as measured by DLS technique. The spectrum of the synthesized AgNPs was observed at 3 KeV using the EDX. On the other hand, FTIR analysis of the green synthesized AgNPs showed the presence of alcohols, phenolics, mono-substituted alkynes, aliphatic primary amines, sodium salt, amino acid, or SiOH alcohol groups. The antimicrobial studies of the formed AgNPs showed positive activity against most of the studied human pathogenic bacteria with varying degrees. Finally, the evaluation of the cytotoxic effect of the green synthesized AgNPs were done using two types of cell lines, human breast cancer cell line (MCF-7) and human colon carcinoma cell line (HCT-116). The results revealed the concentration has a direct correlation with cell viability. The 50% inhibitory concentration (IC_{50}) of MCF-7 cell line was in of 23.5 ± 0.97 μL/100 μL, whereas the HCT-116 cell line was in 37.48 ± 5.93 μL/100 μL.

1. Introduction

The development of antibiotic-resistant pathogenic microbes is a dangerous and prevalent case that threatens public health. Therefore, it is important to focus on effective alternative therapeutic agents, especially those obtained from natural sources, since they are reliable, eco-friendly, non-toxic, and have fewer side effects (Ibraheem et al., 2012, 2016; Hamed et al., 2017). One potential approach is based on bio-synthesis (AgNPs) using biological waste products. Recently, the production of bio-nano particles especially AgNPs has received enormous attentiveness due to its good and potential physicochemical characteristics and the possibility of applications (Alsamhary, 2020; Abdel-Raouf et al., 2019). In contrast to chemical methods, the green nanoparticles are eco-friendly, lower coast, stable for a long time and have the ability to yield a wide variety of formes (spheres, prisms, or plates) with sizes ranging from 1 to 100 nm (Basavegowda and Lee, 2013; Abdel-Raouf et al., 2017a, 2017b). Combination of the small size and high surface-to-volume ratio is the reason behind the effectiveness of nanoparticles (Morones, et al., 2005). Due to their versatile properties, nanoparticles can be employed in several fields, medicine being one of them. One of the applications of nanoparticles involves utilizing them as alternatives to antibiotics. It can be said that antibiotic-resistant strains emerged due to the misuse of antibiotics, and for this reason, multidrug-resistant bacteria have become a worldwide problem (Khameneh, et al., 2016). According to the World Health Organization (2017) Global Antimicrobial Surveillance System, the most reported antibiotic-resistant

* Corresponding authors at: Department of Biology, College of Science and Humanities in Al-Kharj, Prince Sattam bin Abdulaziz University, Al-Kharj 11942, Saudi Arabia (N. Abdel-Raouf).

E-mail addresses: manalk@Ksu.edu.sa (M.M. Alkhulaifi), jamilahamidd@gmail.com (J.H. Alshehri), modhialwehaibi@gmail.com (M.A. Alwehaibi), mawad@ksu.wedu.sa (M.A. Awad), n.alenazi@psau.edu.sa (N.M. Al-Enazi), nasldosari@ksu.edu.sa (N.S. Aldosari), ashrafah76@yahoo.com (A.A. Hatamleh), neveenabdelraouf@gmail.com (N. Abdel- Raouf).

Peer review under responsibility of King Saud University.

Production and hosting by Elsevier

https://doi.org/10.1016/j.sjbs.2020.09.031
1319-562X/

bacteria are *Escherichia coli*, *Klebsiella pneumonia*, *Staphylococcus aureus*, *Streptococcus pneumoniae*, and *Salmonella* spp. Another application of nanotechnology in the field of medicine involves assessment of cytotoxic activity of green synthesized nanoparticles. According to a study conducted on the global burden of cancer worldwide using the GLOBOCAN 2018, there was an estimated 18.1 million new cancer cases and 9.6 million cancer-related deaths in 2018. Therefore, it is necessary to discover new therapeutic agents to counter this incidence and mortality (Bray et al., 2018). *Citrus limon* peels and in particular flavonoid compounds from citrus peel have been identified as agents with utility in the treatment of cancer. This work provides the anticancer potential found within the citrus peel. Historical studies have identified a number of cellular processes that can be modulated by citrus peel flavonoids including cell proliferation, cell cycle regulation, apoptosis, metastasis, and angiogenesis. More recently, molecular studies have started to elucidate the underlying cell signaling pathways that are responsible for the flavonoids' mechanism of action. These growing data support further research into the chemopreventative potential of citrus peel extracts, and purified flavonoids in particular (Koolaji et al., 2020). In this study, we aimed to investigate the green synthesis of silver nanoparticles using natural sources, such as limon peel extract (*Citrus limon*), and to evaluate their antibacterial properties as well as cytotoxic effects.

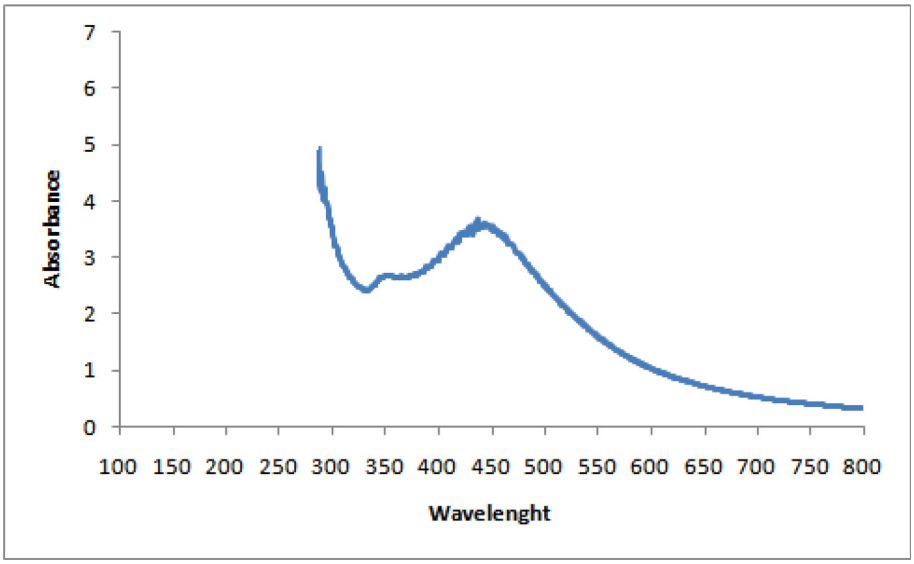

Fig. 1. UV–visible absorption spectra of AgNPs synthesized by LPE. The absorption spectrum of AgNPs exhibited a broad peak at wavelengths of 350–550 nm.

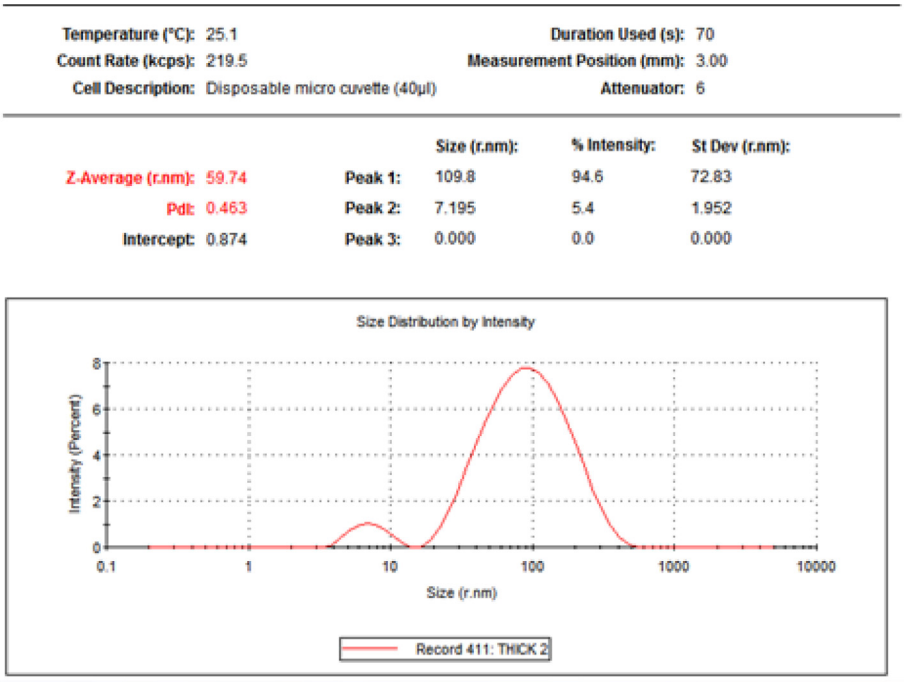

Fig. 2. Size distribution of synthesized AgNPs by Dynamic light scattering (DLS) analysis.

2. Materials and methods

2.1. Collection of Cetrus limon peels and preparation of extract

The *Cetrus limon* peels were collected and cleaned thoroughly using distilled water to remove the dust particles adhering to the surface of the fruit peel. Seventy grams of peels were transferred into 50 mL of boiled distilled water and left to boil for 10 min. The extract obtained was filtered through No. 11.0 cm filter paper, and then, it was stored at 4 °C for further use.

2.2. Green synthesis of AgNPs using Cetrus limon peel extract

Green synthesis of AgNPs involved the addition of 0.008 g (1 mM) silver nitrate ($AgNO_3$) to 50 mL of distilled water, and then,

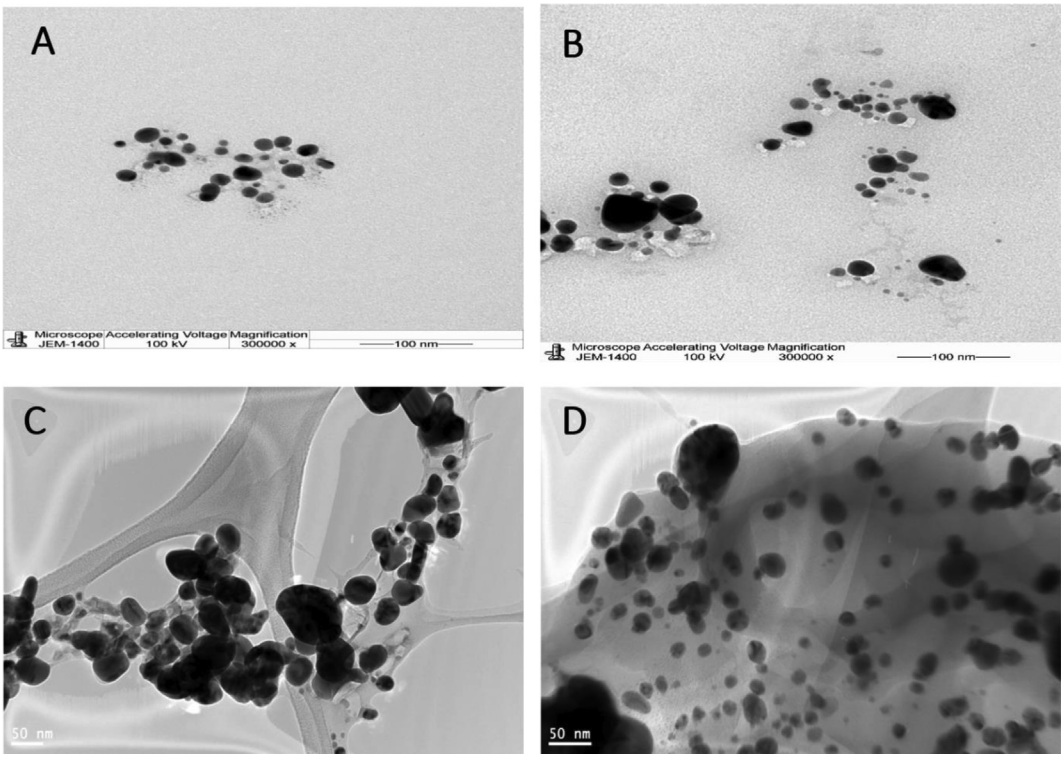

Fig. 3. TEM images (A-D) of the AgNPs synthesized by AgNPs. The shape of AgNPs was spherical, the voltage of 100 kV.

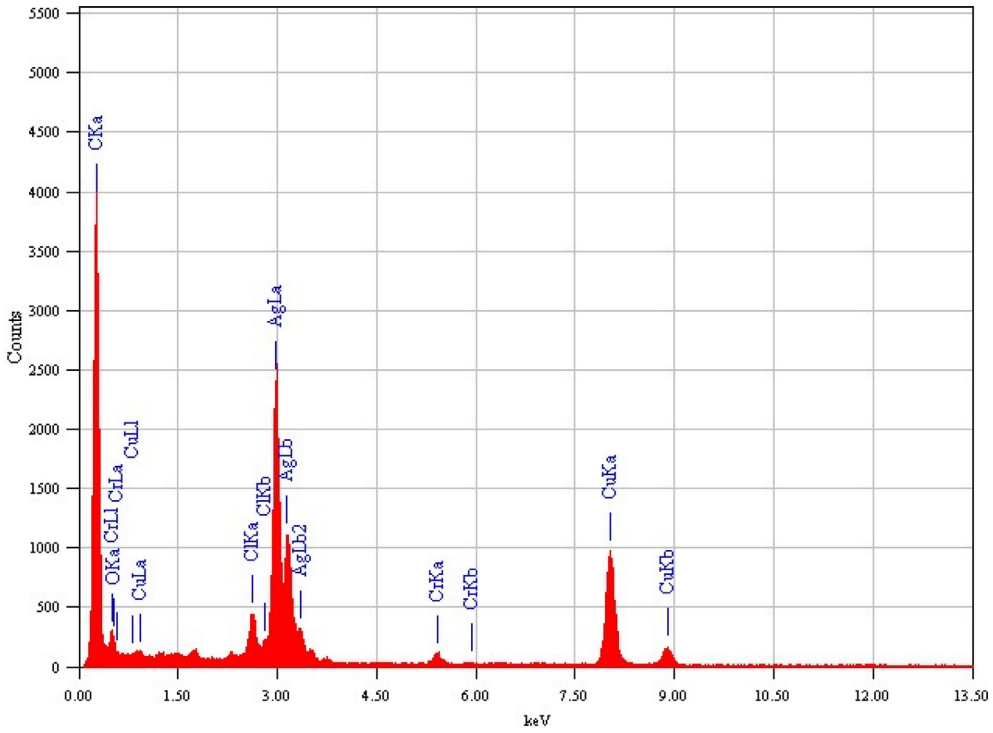

Fig. 4. Energy dispersive x-ray (EDX) spectrum of the synthesized AgNPs.

the solution was stirred with magnetic stirrer for 15 min at 45 °C at 1100 rpm. Then, 5 mL of the *C. limon* peels extract (LPE) was added.

2.3. Characterization of silver nanoparticles

2.3.1. Visible observation

Color change of the mixture to brown color indicates the formation of AgNPs.

2.3.2. UV–Visible spectrophotometry

The green synthesized AgNPs were analyzed with the help of UV–Visible spectrophotometer Libra S60PC.The typical optical spectrum for AgNPs is in the range 350–550 nm (Singh and Vidyasagar 2014).

2.3.3. Dynamic light scattering evaluation

For the size evaluation, the instrument used was Zetasizer Nano ZS (Malvern Instrument Limited, UK). Three milliliters of the AgNPs

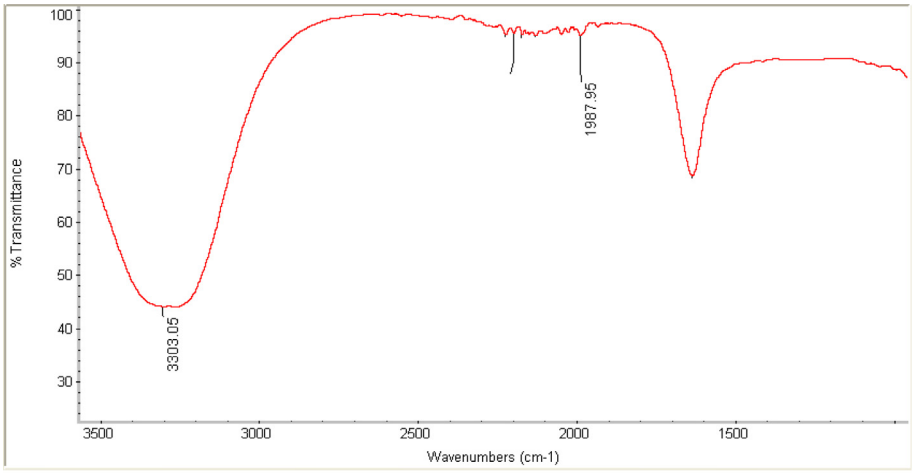

(a)

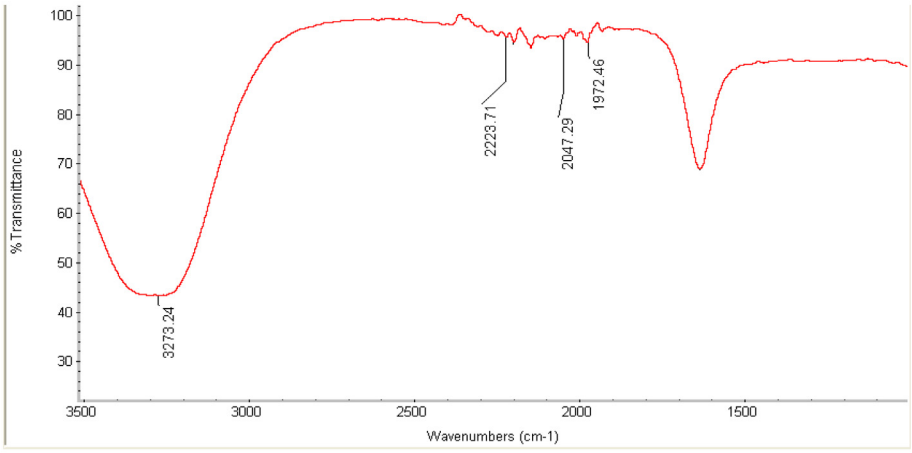

(b)

Fig. 5. Fourier-transform infrared spectroscopy (FTIR) result analysis of AgNPs synthesized by LPE. X-axis represent the spectra (cm^{-1}) and Y-axis represent Present (%) transmission. (a) LPE, (b) AgNPs.

Table 1
The antimicrobial effect of the synthesized LPE AgNPs [inhibition zone measured in millimeter (mm)].

Agent Bacteria	LPE, AgNPs and Referenced Antibiotics inhibition zone (mm)							
	LPE	AgNPs	F	FOS	TE	FEP	MXF	LEV
Salmonella typhimurium	0	33	23.5	21	18	23.5	30	30
E. coli	0	35	23	30	19	17	33	30
A. baumannii	0	15	10	9	18	6	28	31
P. aeruginosa	0	30	7	19	8	7	15	20
P. vulgaris	0	12	18	11	11.5	9	26	23
S. aureus	0	35	33	23	26	24	32	27.5

LPE: The *Citrus limon* peels extract (50 μg); **AgNPs**: The LPE synthesized nanoparticles (50 μg); **F**: Nitrofurantoin (100 μg); **FOS**: Fosfomycin (50 μg); **TE**: Tetracycline (30 μg); **FEP**: Cefepime (30 μg); **MXF**: Moxifloxacin (5 μg); **LEV**: Levofloxacin (5 μg). The used doses were the effective doses as recommended by WHO.

from the LPE were filtered through 0.20 μm pore sized syringe, and then, the solution was analyzed.

2.3.4. Transmission electron microscopy (TEM)

The morphology of the green synthesized AgNPs was examined using TEM. A drop of AgNPs solution was loaded on carbon-coated copper grid and the solvent was allowed to evaporate. The TEM micrograph images were captured using JEM-1400(Jeol Ltd, Japan) with an accelerating voltage of 100 kV.

2.3.5. Energy dispersive x-ray equipped with TEM

A drop of the sample was loaded on the carbon-cupper coated grid and left to dry. The elemental composition of the synthesized AgNPs was evaluated using the energy dispersive x-ray analyzer (JEM-2100F 200 kV, Joel Ltd, Japan).

2.3.6. Fourier-transform infrared spectroscopy

FTIR analysis was conducted using Thermo 6700 (Thermo Fisher Scientific, USA) to determine the functional groups found in the LPE that led to the formation of AgNPs. The absorption bands were observed in the regions of 500–4000 cm^{-1}.

2.3.7. Determination of antibacterial activity of the green synthesized AgNPs

Antibacterial activity test was conducted by a well diffusion method according to Prabhu et al., (2010). The experiment involves testing the produced AgNPs from the LPE against most human pathogenic bacteria, including *Acinetobacter baumannii* (ATCC 19606), *Salmonella typhimurium* (ATCC 14028), *Escherichia coli* (ATCC 35218), *Pseudomonas aeruginosa* (ATCC 27853), *Staphylococcus aureus* (ATCC 25923), and *Proteus vulgaris* (ATCC 49132). The *Citrus limon* peels AgNPs (50 μg) were tested *in vitro* against the tested pathogenic bacteria compared to sex referenced antibiotics. These were Nitrofurantoin (100 μg); Fosfomycin (50 μg); Tetracycline (30 μg); Cefepime (30 μg); Moxifloxacin (5 μg) and Levofloxacin (5 μg). The used doses were the effective doses as recommended by WHO

2.3.8. Analysis of cytotoxic effect of the AgNPs

MCF-7 cells (human breast cancer cell line) and HCT-116 cells (human colon carcinoma cell line) were obtained from VACSERA Tissue Culture Unit. Dimethyl sulfoxide (DMSO), crystal violet, and trypan blue dye were purchased from Sigma (St. Louis, Mo., USA). Fetal bovine serum, DMEM, RPMI-1640, HEPES buffer solution, L-glutamine, gentamycin, and 0.25% Trypsin-EDTA were purchased from Lonza. Crystal violet stain (1%) composed of 0.5% (w/v) crystal violet and 50% methanol dissolved in ddH_2O and filtered through a Whatmann No.1 filter paper. The cytotoxicity test was conducted according the method described by Mosmann, (1983) and Riyadh et al., (2015).

2.4. Statistical analysis

The standard deviation of the mean was calculated according to Lee et al (2015).

3. Results

3.1. Visible observation and UV–visible spectrophotometry results

The formation of the green synthesized AgNPs from the LPE was visually confirmed via color change after 15 min. Analysis with UV–visible spectrophotometer at wavelengths of 350–550 nm showed the formation of AgNPs as shown in Fig. 1.

3.2. Dynamic light scattering results

The average size of AgNPs synthesized using LPE was found to be 59.74 nm as measured by DLS technique as shown in Fig. 2.

3.3. Transmission electron microscop results

As shown in the TEM images shown in Fig. 3a-d, most of the AgNPs were observed to be spherical, and few agglomerated AgNPs were also observed.

3.4. Energy dispersive x-ray analysis

The spectrum of the synthesized AgNPs was observed at 3 KeV using the EDX as shown in Fig. 4.

3.5. Fourier-transform infrared spectroscopy results

The LPE showed absorption peaks at 3303.05, 2198.40, and 1987.95 cm^{-1} (Fig. 5a). While the green synthesized AgNPs showed absorption peaks at 3273.24, 2223.71, 1972.46, and 2047.29 cm^{-1}(Fig. 5b).

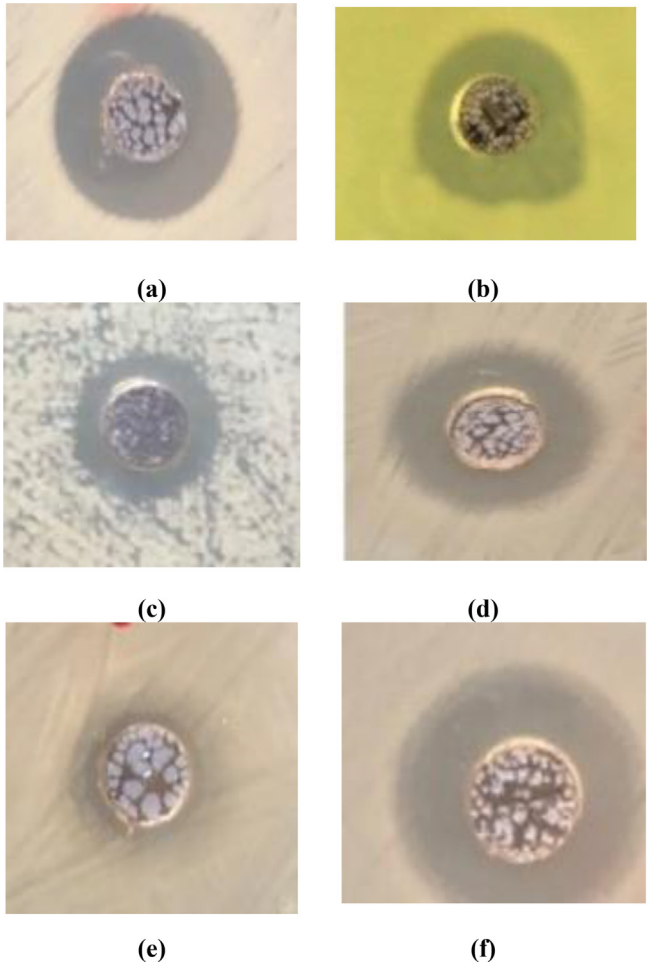

Fig. 6. The inhibition zones representing the antibacterial activity of the synthesized AgNPs against: (a) *S. aureus*; (b) *P. aeruginosa*; (c) *A. baumannii*; (d) *S. typhimurium*; (e) *P. vulgaris* and (f) *E. coli.*

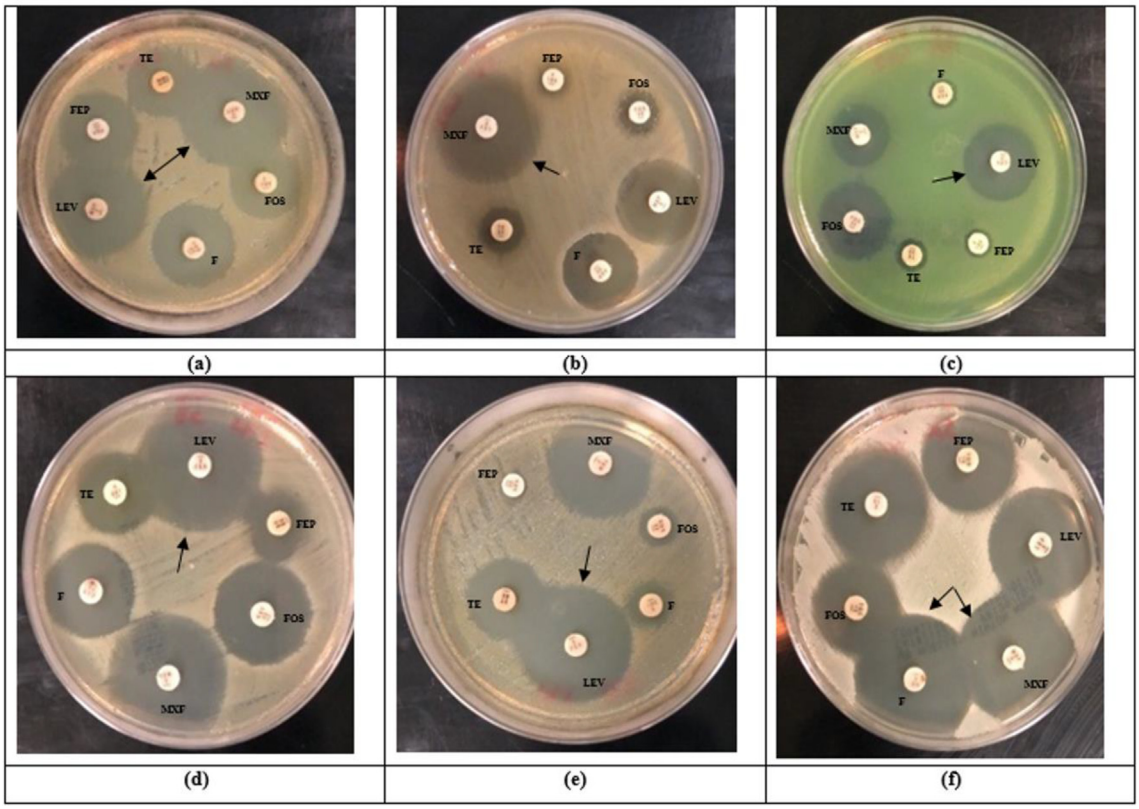

Fig. 7. The antimicrobial activities of the referenced antibiotics against: (a) *S. typhimurium*; (b) *P. vulgaris*; (c) *P. aeruginosa*; (d) *E. coli*; (d) *A. baumannii*; and (f) *S. aureus*. *The arrows represent the maximum inhibition zones by average for each bacterium. **F**: Nitrofurantoin (100 μg); **FOS**: Fosfomycin)50 μg); **TE**: Tetracycline (30 μg); **FEP**: Cefepime (30 μg); **MXF**: Moxifloxacin (5 μg); **LEV**: Levofloxacin (5 μg).

3.6. Determination of the antibacterial activity of the green synthesized silver nanoparticles from the limon peels extract

The obtained results of the practical experiment showed that the LPE extract alone had no anti-bacterial effect (Table 1). While the treatment with the synthase LPE silver nanoparticles showed an inhibitory effects against two types of the bacteria, namely *E. coli* (35 mm) and *S. aureus* (35 mm) (Fig. 6). As this antibacterial effect was higher than that of the reference six antibiotics used (Fig. 7). On the other hand, the treatment with silver nanoparticles extracted from the limen peel showed a different effect compared with the antibiotics used against the remained four bacterial species used in the experiment.

3.7. Cytotoxic effect of the synthesized AgNPs

The evaluation of the cytotoxic effect of the green synthesized AgNPs were done using two types of cell lines, human breast cancer cell line (MCF-7) and human colon carcinoma cell line (HCT-116). The results raveled the concentration has a direct correlation with cell viability as shown in Fig. 8 and Tables 2&3. The 50% inhibitory concentration (IC_{50}) of MCF-7 cell line was in of 23.5 ± 0.9 7 μL/100 μL, whereas the HCT-116 cell line was in 37.48 ± 5. 93 μL/100L.

4. Discussion

The present study demonstrated the green biosynthesis of AgNPs using extract of *Citrus limon* peels, that were treated with 1 mM $AgNO_3$.The colorless $AgNO_3$ solution started turning brown after 15 min; this change could possibly be due to the reduction of Ag ions to silver nanoparticles (Ahmad et al., 2003). For characterization, UV–visible spectrophotometry revealed the maximum peak of the AgNPs at 437 nm; the peak was due to the excitation of the surface plasmon resonance. During the DLS evaluation, the semi-broad peak of the green synthesized AgNPs from LPE (59.74 r.nm) indicated variation in size or an aggregated structure of metal nanoparticles as shown in Fig. 2. The Pdi of 0.463 indicated mono-dispersed nanoparticles (Stetefeld et al., 2012).

TEM images confirmed the existing of spherical and rod-like shaped nanoparticles, as seen in Fig. 3. The results also showed an aggregated structure of the silver nanoparticles; the aggregation could be due to the layer (capping agents) covering the NPs, which causes the NPs to be attached to each other resulting in decreased space between the NPs. These results corroborated with those obtained from UV–visible spectrophotometry and DLS analysis. From the EDX analysis, the absorption peak was observed at 3 KeV indicating the presence of a silver element (Velmurugan et al., 2013). The presence of copper and carbon could be due to the grid's composition. Other signals were also observed indicating the presence of oxygen in the range of 0.0 – 1.5 KeV, chlorine was observed near 3 KeV, and chromium was seen in the range of 0.0 – 6.0 KeV; thus, these could also be components of the peel extract.

In FTIR, LPE revealed several peaks at 3303.05, 2198.40, and 1987.95 cm^{-1}. Peak 3303.05 cm^{-1}may correspond to alcohols, phenolics, mono-substituted alkynes, aliphatic primary amines, sodium salt, amino acid, or SiOH alcohol. Peak 2198.40 cm^{-1}may correspond to NH_3 or alkynes. Peak 1987.95 cm^{-1} may correspond to cumulated alkenes, indicating a typical aromatic benzenoid compound. The green synthesized AgNPs showed absorption peaks at 3273.24, 2223.71, 1972.46, and 2047.29 cm^{-1}. The peak

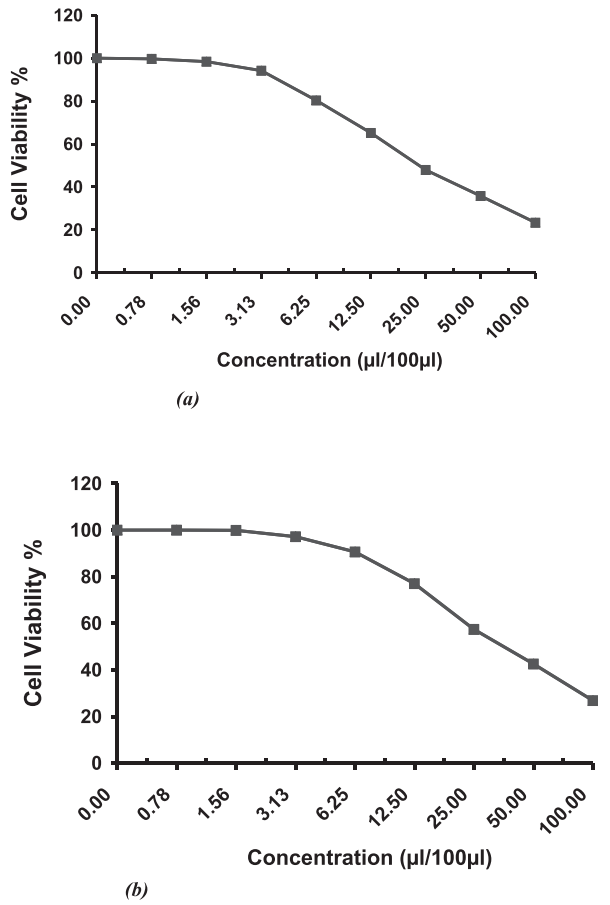

Fig. 8. (a) Cytotoxic effect of AgNPs on human breast cancer cell line (MCF-7), (b) Cytotoxic effect of AgNPs on human colon carcinoma cell line (HCT-116).

3273.24 cm^{-1} may represent alcohols, phenolics, mono-substituted alkynes, aliphatic primary amines, sodium salt, amino acid, or SiOH alcohol. The peak 2223.71 cm^{-1} could correspond to alkynes or ammonium. Peak 1972.46 cm^{-1}maycorrespond to cumulated alkenes, indicating a typical aromatic benzenoid compound. Peak 2047.29 cm^{-1}could correspond to NH_3 (Silverstein et al., 2005). From the comparison between the spectra of the LPE and the green synthesized AgNPs as shown in Fig. 5, the shifts in the positions of the peaks indicated the presence of the functional groups that reduced the silver ions to silver nanoparticles.

Regarding the antimicrobial activity of the prepared AgNPs, the results showed varying degrees of antibacterial activity against human pathogenic bacteria. Based on the results presented in Table 1 and Fig. 6, it is elucidated that these nanoparticles have significant antimicrobial behavior against the tested Gram-negative (E. coli, Salmonella typhimurium and P. aeruginosa) and Gram-positive (S. aureus) bacteria. Based on the inhibitory and bactericidal behavior of the nanoparticles, it was revealed that these nanoparticles are able to inhibit the growth of microbial strains when used in very low concentrations. The antibacterial effect for these particles might be due to the ability of the AgNPs to enhance the permeability of the cell membrane, formation of free radicals, and interaction with thiol groups, prevent DNA replication, affect cellular signaling, and prevent biofilm formation (Rai et al., 2012). Four types of mechanisms have been proposed to interpreting the mechanism of antimicrobial activity of AgNPs, these were; (1)Interaction of AgNPs with cell membranes, alterations in the membrane permeability, and perturbation of respiratory chain enzymes; (2)Gradual diffusion of nanoparticles into the cells, which could both adversely affect the activity of cellular enzymes and restrict the transcription process by conjugation of silver particles to DNA; (3) Leakage of subcellular components as a result of nanoparticles interaction with the plasma membrane leading to cell death and (4) Generation of free radicals when the cell membrane is affected by silver ions (Prabhu and Poulose, 2012; Rizzello and Pompa, 2014).

For the cytotoxicity evaluation, different concentrations of the AgNPs were used. As shown in Tables 2 and 3, by increasing the concentration of the AgNPs, the cell viability decreased (Fig. 8), resulting in IC_{50} of 23.5 ± 0.97 µL/100 µL for MCF-7 and IC_{50} of 37.48 ± 5.93 µL/100 µL for HCT-116. The possible cytotoxic effect might be attributed to the ability of AgNPs to stimulate reactive oxygen species generation in the cellular components, resulting in cell death (Venugopal et al., 2017). It has been postulated that AgNPs interact with mitochondria and disrupt the cellular electron transfer chain function leading to an increase in the ROS level (Park et al., 2010; Singh and Ramarao, 2012). Consequently, the oxidative stress generated by ROS could be considered as a main toxicity mechanism of AgNPs against cells. The elevated anticancer activity of the AgNPs could be attributed to a synergy between AgNPs and the covering polyphenols. It is proposed that the superior cytotoxicity of AgNPs against cancerous cells occurs owing to the highest uptake of nanoparticles by these cells rather than healthy cells, given that cancerous cells have an abnormal metabolism and high proliferation rate, which in turn makes them more vulnerable (Cairns et al., 2011). The simultaneous effect of AgNPs and polyphenols not only increases the ROS generation but also inhibits the transcription process. It is noteworthy that antioxidants such as polyphenols show cytotoxicity only against nonhealthy cells (Li et al., 2006). This report is in good agreement with the data in the literature, which report the concentration-dependent toxicity of nanoparticles, particularly at lower levels (Park et al., 2010; Palaniappan, et al., 2015; Dhand, et al., 2016). It seems that the prominent cell death mechanism is conjugation of nanoparticles with cells and change in the permeability of plasma membrane, which leads to free-radical and ROS generation. This assumption is further augmented by the emergence of pigments (such as beta carotene) in the tested bacteria as a defense mechanism against the oxidative stress.

Table 2
Cytotoxic effects of prepared LPE AgNPs on MCF-7 cell lines.

Sample conc. (µL/100 µL)	Viability% (Mean ± SD)	Inhibitory %
100	23.37 ± 1.68	76.63
50	35.78 ± 1.14	64.22
25	47.95 ± 1.76	52.05
12.5	65.17 ± 2.29	34.83
6.25	80.35 ± 1.20	19.65
3.125	94.20 ± 1.68	5.80
1.56	98.42 ± 1.14	1.58
0.78	99.68 ± 0.56	0.32
0	100 ± 0.00	0

Table 3
Cytotoxic effect of the prepared LPE AgNPs on HCT-116 cell lines.

Sample conc. (µL/100 µL)	Viability% (Mean ± SD)	Inhibitory %
100	26.82 ± 1.42	73.18
50	42.56 ± 2.79	57.44
25	57.42 ± 5.36	42.58
12.5	77.01 ± 4.19	22.99
6.25	90.62 ± 2.79	9.38
3.125	97.17 ± 1.90	2.83
1.56	99.91 ± 0.16	0.09
0.78	100 ± 0.00	0.00
0	100 ± 0.00	0

5. Conclusion

Silver nanoparticles (AgNPs) are of great interest due to their unique and controllable characteristics. A significant improvement in the cytotoxicity characteristics of the green synthesized Ag nanoparticles against a cancerous cell line. These findings imply that the synthesized nanoparticles using green nanotechnology could be an ideal strategy to combat cancer and infectious diseases. The synthesized AgNPs proved to possess improved anticancer, antimicrobial activity in comparison with the extract. The method of AgNPs synthesis introduced in this study, therefore, holds great potential as a simple, low-cost, and environmentally-friendly approach for producing value-added products from waste material. The synthesized AgNPs exhibited selective cytotoxicity toward the cancerous cell line when compared to their effect on the normal cell line tested. These findings are very promising in utilizing the biological effects of the AgNPs synthesized using walnut green husk extract.

6. Recommendation

In the future, we recommend optimizing the conditions when synthesizing AgNPs, as well as understanding the mode of action and determining the toxic effects on animals, to be able to employ the AgNPs in the field of medicine as a possible therapeutic agent.

Acknowledgements

The authors extend their appreciation to the Deanship of Scientific Research at King Saud University for funding this work through the Undergraduate Student's Research Support Program, Project no. (URSP-3-18-107). The researchers are also thankful to the Deanship of Scientific Research and RSSU at King Saud University for their technical support. The researchers would like to thank the departments of Physics, Chemistry, Biochemistry, Botany and Microbiology.

References

Abdel-Raouf, N., Al-Enazi, N.M., Ibraheem, B.M., 2017a. Green biosynthesis of gold nanoparticles using *Galaxaura elongata* and characterization of their antibacterial activity. Arabian J. Chem. 10, S3029–S3039.

Abdel-Raouf, N., Al-Enazi, N.M., Ibraheem, B.M.I., Alharbi, R.M., Alkhulaifi, M.M., 2019. Biosynthesis of silver nanoparticles by using of the marine brown alga Padina pavonia and their characterization. Saudi Journal of Biological Sciences. 26 (6), 1207–1215.

Abdel-Raouf, N., Al-Enazi, N.M., Ibraheem, I.B.M., Alharbi, R.M., Alkhulaifi, M.M., 2017b. Bactericidal efficacy of Ag and Au nanoparticles synthesized by the marine alga *Laurencia catarinensis*. International Journal of Pharmaceutical Research & Allied Sciences 6 (2), 213–226.

Ahmad, A., Mukherjee, P., Senapati, S., Mandal, D., Khan, M.I., Kumar, R., Sastry, M., 2003. Extracellular biosynthesis of silver nanoparticles using the fungus *Fusarium oxysporum*. Colloids and surfaces B: Biointerfaces. 28 (4), 313–318.

Alsamhary, K.I., 2020. Eco-friendly synthesis of silver nanoparticles by Bacillus subtilis and their antibacterial activity. Saudi Journal of Biological Sciences. 27 (8), 2185–2191.

Basavegowda, N., Lee, Y.R., 2013. Synthesis of silver nanoparticles using *Satsuma mandarin* (Citrus unshiu) peel extract: a novel approach towards waste utilization. Materials Letters. 109, 31–33.

Bray, F., Ferlay, J., Soerjomataram, I., Siegel, R.L., Torre, L.A., Jemal, A., 2018. Global cancer statistics 2018: GLOBOCAN estimates of incidence and mortality worldwide for 36 cancers in 185 countries. CA Cancer J Clin. 68 (6), 394–424.

Cairns, R.A., Harris, I.S., Mak, T.W., 2011. Regulation of cancer cell metabolism. Nat Rev Cancer. 11 (2), 85–95.

Dhand, V., Soumya, L., Bharadwaj, S., Chakra, S., Bhatt, D., Sreedhar, B., 2016. Green synthesis of silver nanoparticles using *Coffea arabica* seed extract and its antibacterial activity. Mater Sci Eng C Mater Biol Appl. 58, 36–43.

Hamed, S.M., Abdel-Alim, M.M., Abdel-Raouf, N., Ibraheem, I.B.M., 2017. Biosynthesis of silver chloride nanoparticles using the cyanobacterium *Anabaena variabilis*. Life Science Journal. 14 (6), 25–30.

Ibraheem, I.B.M., Al-Othman, M.R., Abdel-Raouf, N., 2012. Cyanobacterial extra-metabolites against some pathogenic bacteria. African Journal of Microbiology Research. 6 (38), 6720–6725.

Ibraheem, I.B.M., Abd Elaziz, B.E.E., Saad, W.F., Fathy, W.A., 2016. Green biosynthesis of silver nanoparticles using marine red algae *Acanthophora specifera* and its antimicrobial activity. Journal of Nanomedicine & Nanotechnology. 7, 409. https://doi.org/10.4172/2157-7439.1000409.

Khameneh, B., Diab, R., Ghazvini, K., Bazzaz, B.S.F., 2016. Breakthroughs in bacterial resistance mechanisms and the potential ways to combat them. Microbial Pathogenesis. 95, 32–42.

Koolaji, N., Shammugasamy, B., Schindeler, A., Dong, Q., Dehghani, F., Valtchev, P., 2020. *Citrus* peel flavonoids as potential cancer prevention agents. Current Developments. Nutrition. 4 (5). https://doi.org/10.1093/cdn/nzaa025.

Lee, D.K., In, J., Lee, S., 2015. Standard deviation and standard error of the mean. Korean Journal of Anesthesiol. 68 (3), 220–223.

Li, L., Tsao, R., Yang, R., Liu, C., Zhu, H., Young, J.C., 2006. Polyphenolic profiles and antioxidant activities of heartnut (*Juglans ailanthifolia Varcordiformis*) and Persian walnut (*Juglans regia* L.). J Agric Food Chem. 54 (21), 8033–8040.

Morones, J.R., Elechiguerra, J.L., Camacho, A., Holt, K., Kouri, J.B., Ramírez, J.T., Yacaman, J.M., 2005. The bactericidal effect of silver nanoparticles. Nanotechnology. 16 (10), 2346–2353.

Mosmann, T., 1983. Rapid colorimetric assay for cellular growth and survival: application to proliferation and cytotoxicity assays. Journal of Immunological Methods. 65 (1–2), 55–63.

Palaniappan, P., Sathishkumar, G., Sankar, R., 2015. Fabrication of nano-silver particles using *Cymodocea serrulata* and its cytotoxicity effect against human lung cancer A549 cells line. Spectrochim Acta A Mol Biomol Spectrosc. 138, 885–890.

Park, E.J., Yi, J., Kim, Y., Choi, K., Park, K., 2010. Silver nanoparticles induce cytotoxicity by a Trojan-horse type mechanism. Toxicol In Vitro. 24 (3), 872–878.

Prabhu, N., Divya, T.R., Yamuna, G., 2010. Synthesis of silver phytonanoparticles and their antibacterial efficacy. Digest J. Nanomater. Biostruct. 5, 185–189.

Prabhu, S., Poulose, E.K., 2012. Silver nanoparticles: mechanism of antimicrobial action, synthesis, medical applications, and toxicity effects. Int Nano Lett. 2 (1), 32–41.

Rai, M.K., Deshmukh, S.D., Ingle, A.P., Gade, A.K., 2012. Silver nanoparticles: the powerful nanoweapon against multidrug-resistant bacteria. Journal of Applied Microbiology. 112, 841–852.

Riyadh, S.M., Gomha, S.M., Mahmmoud, E.A., Elaasser, M.M., 2015. Synthesis and Anticancer Activities of Thiazoles, 1,3-Thiazines, and Thiazolidine Using Chitosan-Grafted-Poly(vinylpyridine) as Basic Catalyst. Heterocycles. 91 (6). 1227-0-1243.

Rizzello, L., Pompa, P.P., 2014. Nanosilver-based antibacterial drugs and devices: mechanisms, methodological drawbacks, and guidelines. Chem Soc Rev. 43 (5), 1501–1518.

Silverstein, R., Webster, F., Kiemle, D., 2005. Spectrometric identification of organic compounds. John Wiely & Sons Inc, New York, pp. 71–143.

Singh, P.S., Vidyasagar, G.M., 2014. Biosynthesis, characterization, and antidermatophytic activity of silver nanoparticles using Raamphal Plant (*Annona reticulata*) aqueous leaves extract. Indian Journal of Materials Science. https://doi.org/10.1155/2014/412452.

Singh, R.P., Ramarao, P., 2012. Cellular uptake, intracellular trafficking and cytotoxicity of silver nanoparticles. Toxicol Lett. 213 (2), 249–259.

Stetefeld, J., McKenna, S.A., Patel, T.R., 2012. Dynamic light scattering: a practical guide and applications in biomedical sciences. Biophysical Reviews. 8 (4), 409–427.

Velmurugan, P., Lee, S.M., Iydroose, M., Lee, K.J., Oh, B.T., 2013. Pine cone-mediated green synthesis of silver nanoparticles and their antimicrobial activity against agricultural pathogens. Applied Microbiology and Biotechnology. 97 (1), 361–368.

Venugopal, K., Ahmad, H., Manikandan, E., Thanigai Arul, K., Kavitha, K., Moodley, M., Rajagopal, K., Balabhaskar, R., Bhaskar, M., 2017. The impact of anticancer activity upon *Beta vulgaris* extract mediated biosynthesized silver nanoparticles (ag-NPs) against human breast (MCF-7), lung (A549) and pharynx (Hep-2) cancer cell lines. Journal of Photochemistry and Photobiology B: Biology. 173, 99–107.

World Health Organization, 2017. Global priority list of antibiotic-resistant bacteria to guide research, discovery, and development of new antibiotics. World Health Organization, Geneva.